

Growth of $\text{Bi}_4\text{Ti}_{3-x}\text{Zr}_x\text{O}_{12}$ Single Crystal by Floating Zone Method

Tohru Higuchi, Yoshiyuki Moriuchi, Makoto Satake, Takeshi Hattori and Takeyo Tsukamoto

Department of Applied Physics, Tokyo University of Science, 1-3 Kagurazaka, Shinjuku, Tokyo 162-8601, Japan

Fax: 81-3-5228-8241, e-mail: higuchi@rs.kagu.tus.ac.jp

The structural properties of Zr^{4+} -doped $\text{Bi}_4\text{Ti}_3\text{O}_{12}$ ($\text{Bi}_4\text{Ti}_{3-x}\text{Zr}_x\text{O}_{12}$) were firstly studied in single crystal grown by floating zone method. The XRD pattern of the single crystal exhibited the single phase. The intensity of Ti 2p X-ray absorption spectra decreases with increasing Zr^{4+} concentration, indicating that the doped Zr^{4+} ions enter the Ti^{4+} site in $\text{Bi}_4\text{Ti}_3\text{O}_{12}$. The analysis of domain structure of single crystal in the a - b plane with an optical microscope exhibited that the $\text{Bi}_4\text{Ti}_{3-x}\text{Zr}_x\text{O}_{12}$ has a striped 90° domain wall.

Key words: Zr-doped $\text{Bi}_4\text{Ti}_3\text{O}_{12}$ ($\text{Bi}_4\text{Ti}_{3-x}\text{Zr}_x\text{O}_{12}$), single crystal, ceramics, domain structure, floating-zone (FZ) method

1. INTRODUCTION

Ferroelectric thin films have attracted considerable attention because of their use in ferroelectric random access memories (FeRAMs). Most of the attention has been focused on bismuth layer-structured ferroelectrics, such as $\text{Bi}_4\text{Ti}_3\text{O}_{12}$ (BIT) and $\text{SrBi}_2\text{Ta}_2\text{O}_9$ [1-3]. In particular, the BIT exhibits a spontaneous polarization in the a - c plane at an angle of about 4.5° to the a -axis, and exhibits two independently reversible components along the c - and a -axes. The c -axis oriented BIT thin films are expected to be applied to nonvolatile FeRAM device with nondestructive readout operation because of their low dielectric constant and small coercive field. Furthermore, the BIT thin films are considered promising due to their excellent fatigue endurance when used with a Pt electrode.

In recent years, La-doped BIT ($\text{Bi}_{4-x}\text{La}_x\text{Ti}_3\text{O}_{12}$) has been reported as a promising material to solve poor fatigue of BIT. The $\text{Bi}_{4-x}\text{La}_x\text{Ti}_3\text{O}_{12}$ thin film, which was prepared at a low temperature of 650°C , exhibits a relatively large remanent polarization, and superior fatigue endurance was confirmed [4-6]. Such a significant improvement in ferroelectricity has been observed only for $(\text{Bi}_{4-x}\text{La}_x)(\text{Ti}_{3-y}\text{V}_y)\text{O}_{12}$ and $\text{Bi}_4\text{Ti}_{3-y}\text{V}_y\text{O}_{12}$ films. This selective control of each site is named "site-engineering". The effect of the site-engineering technique for BIT has been extensively studied by Watanabe and co-workers [7-10]. They reported that the major contribution of site-engineering for BIT is to adjust the Curie temperature and to suppress the domain pinning. Therefore, understanding structural properties of selective controlled BIT is one of the most important subjects in term of FeRAM applications.

In this study, we have prepared Zr-doped BIT ($\text{Bi}_4\text{Ti}_{3-x}\text{Zr}_x\text{O}_{12}$) single crystal by floating zone (FZ) method and studied its structural properties. The structural properties were characterized by X-ray diffraction (XRD) and X-ray absorption spectroscopy (XAS). The XAS is related directly to the unoccupied DOS [11,12]. This optical process is rather local process, because of the localized core state. It is governed by dipole selection rules so that XAS gives the spectrum related to the site- and symmetry-selected

DOS. The domain structure in the a - b plane of single crystal was also observed by optical microscope.

2. EXPERIMENTAL

The $\text{Bi}_4\text{Ti}_{3-x}\text{Zr}_x\text{O}_{12}$ ceramics were prepared by wet-ball mill method. The mixtures of Bi_2O_3 , TiO_2 and ZrO_2 powders were calcined in air at 750°C for 4h, and then crushed. The crushed powders were pressed into pellets of 17mm in diameter, and then sintered in air at $1000\sim 1050^\circ\text{C}$ for 4 h. The Zr^{4+} concentrations were $x=0\sim 0.045$.

The $\text{Bi}_4\text{Ti}_{3-x}\text{Zr}_x\text{O}_{12}$ single crystal was performed by mean of an infrared radiation furnace equipped with an ellipsoidal mirror and a 1.5 KW halogen lamp. In order to prevent Bi-deficiency, excess Bi_2O_3 of 2.5% and 5.0% at the rate of weight was added to the starting powders. The mixtures were formed into a cylindrical shape in a rubber tube. The formed powders were compressed at a hydrostatic pressure of 500 kgf/cm^2 to form a sample rod of 5~7 mm in diameter and 70 mm in length. The sample rods were sintered in air at 1000°C for 0 wt%, 900°C for 2.5 wt% and 925°C for 5.0 wt%. The sintered rods were used as both a seed and a charge rod, and equipped into a contrivance. The single crystal was grown under the shaft-descent-speed of 1 mm/h, shaft-turning-speed of 20rpm and total flow rate ($\text{Ar}:\text{O}_2=2:1$) of 500 ml/min.

The $\text{Bi}_4\text{Ti}_{3-x}\text{Zr}_x\text{O}_{12}$ ceramics and single crystal were confirmed as being a single phase with BZT structure by the powder XRD analysis. On the other hand, the electronic structure was studied by XAS technique. The XAS spectra were measured at the revolver undulator beamline BL-19B at the Photon Factory (PF) of the High Energy Accelerator Organization (KEK), Tsukuba in Japan. Synchrotron radiation was monochromatized using a varied-line spacing plain grating whose average groove density is 1000 lines/mm. The spectra were measured in a polarized configuration. The XAS spectra were measured by collecting the total fluorescence yield. The total resolution of the experimental system was about 80 meV at $h\nu=500\text{ eV}$.

3. RESULTS AND DISCUSSION

Figure 1 shows the XRD patterns as a function of Zr^{4+} concentration in $\text{Bi}_4\text{Ti}_{3-x}\text{Zr}_x\text{O}_{12}$ ceramics. These XRD patterns exhibited the single phase. These ceramics were used as both a seed and a charge rod.

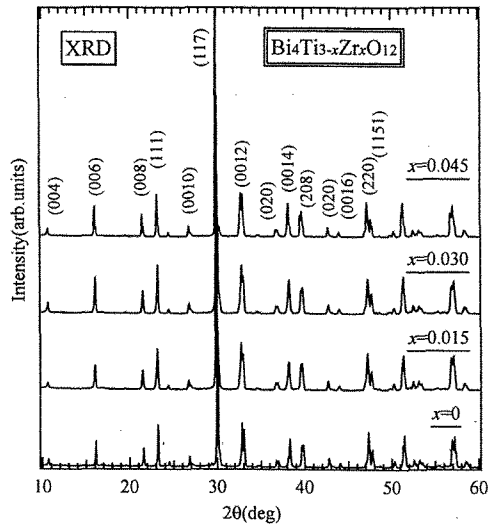


Fig. 1 XRD patterns as a function of Zr^{4+} concentration in $\text{Bi}_4\text{Ti}_{3-x}\text{Zr}_x\text{O}_{12}$ ceramics.

In the preparation of $\text{Bi}_4\text{Ti}_{3-x}\text{Zr}_x\text{O}_{12}$ single crystal by floating zone method, a large problem is Bi vaporization during growth. In this study, we have clarified that the Bi vaporization is possible to prevent by controlling the total flow rate of Ar and O_2 gas. However, just it is inadequate. Therefore, excess Bi_2O_3 of 2.5 wt% and 5.0 wt% at the late weight was added to starting powders to consider bismuth vaporization beforehand. The XRD patterns of $\text{Bi}_4\text{Ti}_{2.955}\text{Zr}_{0.045}\text{O}_{12}$ as a function of Bi-excess are shown in Fig. 2. The XRD patterns exhibit c-axis oriented $\text{Bi}_4\text{Ti}_{2.955}\text{Zr}_{0.045}\text{O}_{12}$ single phase. The Bi-content of 0 wt%-Bi-excess confirmed by EPMA was the composition ratio of 54.18 %, though the Bi-content of 5.0 wt%-Bi-excess was very near value (56.94%) to stoichiometric composition. The photograph of the single crystal is shown in Fig. 3.

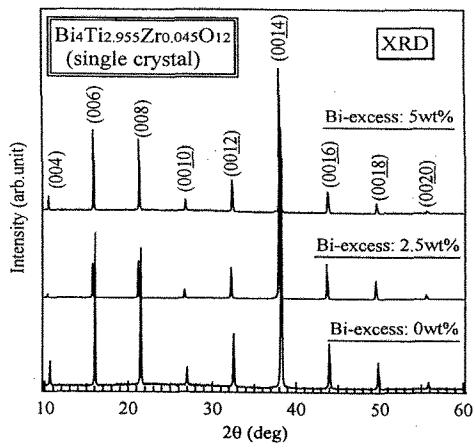


Fig. 2 XRD patterns of $\text{Bi}_4\text{Ti}_{2.955}\text{Zr}_{0.045}\text{O}_{12}$ single crystal grown using excess-Bi ceramics.

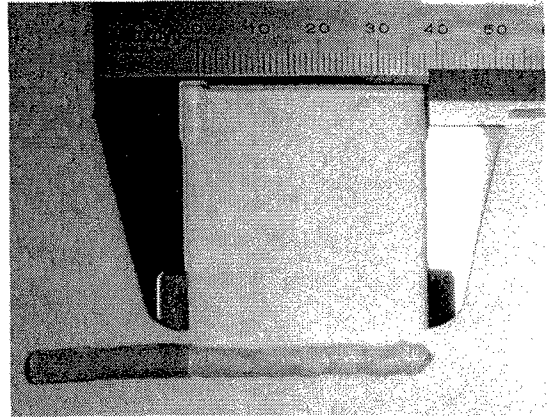


Fig. 3 Photograph of $\text{Bi}_4\text{Ti}_{2.955}\text{Zr}_{0.045}\text{O}_{12}$ single crystal by grown by floating zone method.

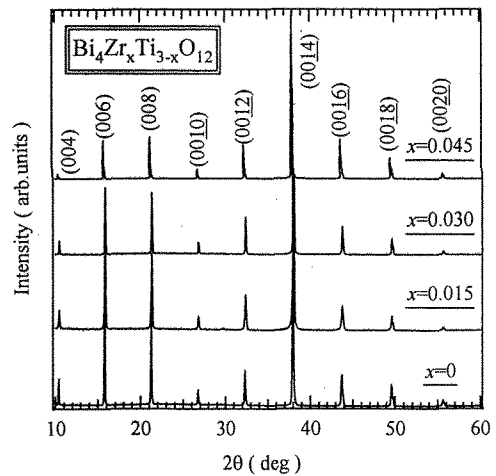


Fig.4 XRD patterns as a function of Zr^{4+} concentration in $\text{Bi}_4\text{Ti}_{3-x}\text{Zr}_x\text{O}_{12}$ single crystal.

Figure 4 shows the XRD patterns as a function of Zr^{4+} concentration in $\text{Bi}_4\text{Ti}_{3-x}\text{Zr}_x\text{O}_{12}$ single crystal. The prepared single crystals exhibited the single phase.

Figure 5 shows the Ti 2p XAS spectra as a function of Zr^{4+} concentration in $\text{Bi}_4\text{Ti}_{3-x}\text{Zr}_x\text{O}_{12}$ single crystal. The Ti 2p XAS spectra correspond to the transition from Ti 2p core level to unoccupied Ti 3d state. The spectra are derived from the two parts of L_3 ($2p_{3/2}$) and L_2 ($2p_{1/2}$). They are split into the t_{2g} - and e_g -subbands by the octahedral ligand field [11]. The intensity of t_{2g} -subband decreases with increasing Zr^{4+} concentration. This results indicates that the doped Zr^{4+} ions enter the Ti^{4+} site of BIT.

Figure 6 shows the O 1s XAS spectra as a function of Zr^{4+} dopant concentration in $\text{Bi}_4\text{Ti}_{3-x}\text{Zr}_x\text{O}_{12}$ single crystal. From the dipole selection rule, it is understood that the O 1s XAS spectra of Ti oxides correspond to transitions from O 1s to the O 2p character hybridized with the unoccupied Ti 3d state [11-14]. The O 1s XAS spectra are normalized by measurement time and beam current. The spectra are derived from the two parts of the t_{2g} - and e_g -subbands of Ti 3d state. The energy separation between the t_{2g} - and e_g -subbands is in good agreement with Fig. 5. The spectral intensities do not depend on

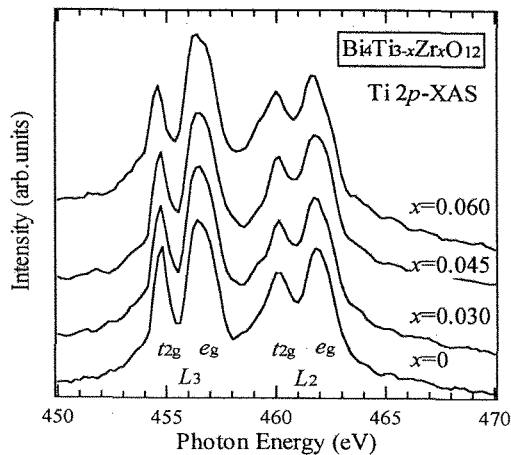


Fig. 5 Ti 2p XAS spectra as a function of Zr^{4+} concentration in $Bi_4Ti_{3-x}Zr_xO_{12}$ single crystals.

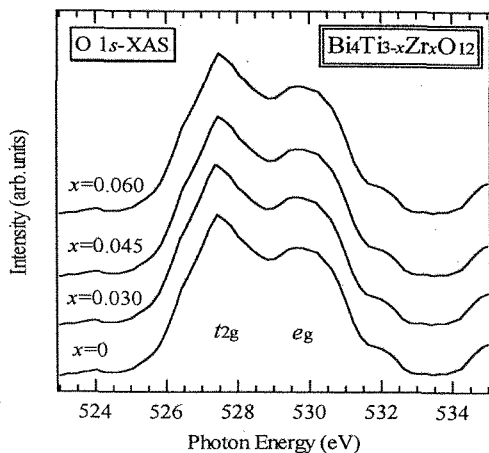


Fig. 6 O 1s XAS spectra as a function of Zr^{4+} concentration in $Bi_4Ti_{3-x}Zr_xO_{12}$ single crystals.

Zr^{4+} concentration. This result indicates that O^{2-} site is not affected by Zr^{4+} doping.

Figure 7 shows the domain structure in the a - b plane of as-grown BIT and $Bi_4Ti_{2.97}Zr_{0.03}Ti_3O_{12}$ single crystals investigated by an optical microscope. This photograph indicates an in-plane domain structure since the spontaneous polarization (P_s) of about $50 \mu C/cm^2$ lies along the a -axis at the angle of about 5° with the a - b plane. The observed photograph exhibits a striped 90° domain wall. The average domain widths of BIT and $Bi_4Ti_{2.955}Zr_{0.045}O_{12}$ single crystals are approximately $10 \mu m$ and $5 \mu m$, respectively. The 90° domain walls are visible with an optical microscope due to the elastic distortion at the boundary, while the 180° domain wall can not be observed. This behavior resembles with La-doped BIT (BLT) single crystal [15-19]. Noguchi and co-workers have reported that the improvement of polarization properties observed for BLT thin films is closely related to the domain structure [16-18]. Such a fact might be also expected for $Bi_4Ti_{3-x}Zr_xO_{12}$.

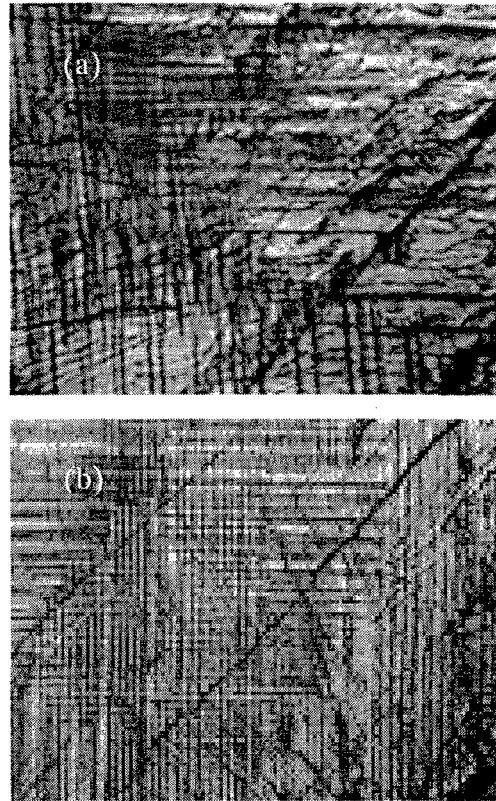


Fig. 7 Domain structures of as-grown (a) BIT and (b) $Bi_4Ti_{2.97}Zr_{0.03}Ti_3O_{12}$ single crystal observed by optical microscope.

4. CONCLUSION

We prepared the $Bi_4Ti_{3-x}Zr_xO_{12}$ ceramics and single crystal and studied their structural properties. The prepared ceramics exhibited the $Bi_4Ti_{3-x}Zr_xO_{12}$ single phase. The intensity of Ti 2p XAS spectra of $Bi_4Ti_{3-x}Zr_xO_{12}$ ceramics decreases with increasing Zr concentration, indicating that the doped Zr ions enter the Ti^{4+} site. On the other hand, the $Bi_4Ti_{2.955}Zr_{0.045}O_{12}$ single crystal was prepared by FZ method. When Bi of ceramics rod is 5.0 wt%-excess, the XRD pattern exhibited the c -axis oriented $Bi_4Ti_{2.955}Zr_{0.045}O_{12}$ single phase. The prepared single crystal exhibited a striped 90° domain structure, and the domain width was approximately $5\sim 10 \mu m$.

ACKNOWLEDGEMENTS

We would like to thank Mr. M. Nanba and S. Izukawa for their useful discussions. This work was partially supported by the Foundation for Materials Science and Technology of Japan (MST Foundation), and the Grant-In-Aid for Scientific Research from the Ministry of Education, Cultures, Sports, Science and Technology.

REFERENCES

- [1] E. C. Subbarao: *Phys. Rev.* **122** (1961) 804.
- [2] S. E. Cummins and L. E. Cross: *Appl. Phys. Lett.* **10** (1967) 14.
- [3] R. W. Wolfe and R. E. Newnham: *J. Electrochem. Soc.* **116** (1967) 832.
- [4] B. H. Park, B. S. Kang, S. D. Bu, T. W. Noh, J. Lee and W. Jo: *Nature* **410** (1999) 682.
- [5] U. Chon, G. Yi and H. M. Jang: *Appl. Phys. Lett.* **78** (2001) 658.
- [6] Y. Hou, X. Xu, H. Wang, M. Wang and S. Shang: *Appl. Phys. Lett.* **78** (2001) 1733.
- [7] T. Watanabe, A. Saiki, K. Saito and H. Funakubo: *J. Appl. Phys.* **89** (2001) 3934.
- [8] E. Tokumitsu, T. Isobe, T. Kijima and H. Ishiwara: *Jpn. J. Appl. Phys.* **40** (2001) 5576.
- [9] T. Watanabe, T. Kojima, T. Sakai, H. Funakubo, M. Osada, Y. Noguchi and M. Miyayama: *J. Appl. Phys.* **92** (2002) 1518.
- [10] T. Watanabe, H. Funakubo, M. Osada, Y. Noguchi and M. Miyayama: *Appl. Phys. Lett.* **80** (2002) 100.
- [11] T. Higuchi, T. Tsukamoto, M. Watanabe, M. M. Grush, T. A. Callcott, R. C. Perera, D. L. Ederer, Y. Tokura, Y. Harada, Y. Tezuka and S. Shin: *Phys. Rev. B* **60** (1999) 7711.
- [12] T. Higuchi, T. Tsukamoto, K. Kobayashi, S. Yamaguchi, Y. Ishiwata, N. Sata, K. Hiramoto, M. Ishigame and S. Shin: *Phys. Rev. B* **65** (2002) 33201.
- [13] T. Higuchi, M. Tanaka, K. Kudoh, T. Takeuchi, Y. Harada, S. Shin and T. Tsukamoto: *Jpn. J. Appl. Phys.* **40** (2001) 5803.
- [14] T. Higuchi, K. Kudoh, T. Takeuchi, Y. Masuda, Y. Harada, S. Shin and T. Tsukamoto: *Jpn. J. Appl. Phys.* **41** (2002) 7195.
- [15] R. Aoyagi, H. Takeda, S. Okamura and T. Shiosaki: *Jpn. J. Appl. Phys.* **40** (2001) 5671.
- [16] Y. Noguchi, I. Miwa, Y. Goshima and M. Miyayama: *Jpn. J. Appl. Phys.* **39** (2000) L1259.
- [17] M. Takahashi, Y. Noguchi and M. Miyayama: *Jpn. J. Appl. Phys.* **41** (2002) 7053.
- [18] M. Soga, Y. Noguchi and M. Miyayama: *Mater. Res. Soc. Jpn.* (2003) in press.

(Received December 23, 2004; Accepted January 31, 2005)